What Is Triggering Ice in Mixed-Phase Clouds: A Process Analysis With ECHAM6.1-HAM2.3 Using the Factorial Method

JGR Atmospheres

RESEARCH ARTICLE
10.1029/2025JD045160

What Is Triggering Ice in Mixed-Phase Clouds: A Process Analysis With ECHAM6.1-HAM2.3 Using the Factorial Method

L. Ickes[1,2], D. Neubauer[2,3], U. Proske[2,4], D. Villanueva[2], and U. Lohmann[2]

[1]Now at Department of Environmental and Energy Sciences, Chalmers University of Technology, Gothenburg, Sweden, [2]Institute for Atmospheric and Climate Science, ETH, Zurich, Switzerland, [3]Now at GeoSphere Austria, Vienna, Austria, [4]Now at Hydrology and Environmental Hydraulics, Wageningen University, Wageningen, The Netherlands

Key Points:

- Sedimentation of ice crystals triggers most of the water-to-ice phase transition in warm mixed-phase clouds (>−25°C)
- Freezing is the least important ice-triggering process in warm mixed-phase clouds (>−25°C) with increasing importance for colder clouds
- The factorial analysis is a suitable framework to analyze the effect of ice-triggering processes and facilitates model intercomparison

Correspondence to:
L. Ickes,
luisa.ickes@chalmers.se

Citation:
Ickes, L., Neubauer, D., Proske, U., Villanueva, D., & Lohmann, U. (2026). What is triggering ice in mixed-phase clouds: A process analysis with ECHAM6.1-HAM2.3 using the factorial method. *Journal of Geophysical Research: Atmospheres*, *131*, e2025JD045160. https://doi.org/10.1029/2025JD045160

Received 13 AUG 2025
Accepted 16 MAY 2026

Abstract Mixed-phase clouds can be found at temperatures between 0 and −38°C and consist of supercooled cloud droplets and ice crystals. The phase of mixed-phase clouds is crucial for the radiation budget, which determines the atmosphere's energy balance. The transition of a supercooled cloud to a mixed-phase or ice cloud is triggered by different processes that form or introduce ice crystals into a supercooled cloud. Once ice crystals are present, they grow at the expense of the cloud droplets due to the Wegener-Bergeron-Findeisen process. This causes a partial or complete glaciation of the mixed-phase cloud. In the global climate model ECHAM6.1-HAM2.3, three trigger processes introduce initial ice crystals into a supercooled stratiform cloud: heterogeneous freezing, sedimentation of ice crystals from upper cloud layers (in-cloud seeding or seeder-feeder process), and vertical transport (vertical diffusion and vertical advection) of ice crystals. The role of these three ice-triggering processes was investigated by conducting a set of simulations and analyzing them using a statistical framework (factorial method). For that framework, the supercooled liquid fraction of a mixed-phase cloud was used as an indicator of the microphysical structure and phase of the cloud. It was found that the sedimentation of the ice crystals is crucial for triggering the ice in mixed-phase stratiform clouds in ECHAM6.1-HAM2.3. Our results affect the model's sensitivity to freezing parameterizations and variations in aerosol-cloud interactions.

Plain Language Summary Clouds are made of tiny water droplets or ice crystals, and some clouds—called mixed-phase clouds—have both. Clouds are important because they affect Earth's climate by influencing how much sunlight is reflected or trapped. But scientists still struggle to understand which mechanisms in these clouds turn water into ice under different meteorological and dynamical conditions. This study used a climate model to test three ways ice might form in this model and the importance of each process: (a) Freezing aided by particles, (b) Falling ice crystals from higher clouds or higher cloud layers (called sedimentation), and (c) Air movements that carry ice crystals up and down (vertical transport). It was shown that sedimentation and vertical transport are important to distribute ice crystals throughout clouds, especially in warmer parts of the mixed-phase range (above −25°C). Freezing only becomes important at colder temperatures (below −30°C). In thicker clouds, ice moves around more, making sedimentation and vertical transport even more important. It is suggested to investigate the matter with other models and complement with observations to derive more conclusions for further model development.

1. Introduction

Clouds influence both incoming and outgoing radiation, and they transport heat and moisture throughout the atmosphere. Due to their role in the global energy and water budget, they are an essential element of the climate system (Chahine, 1992; Quante, 2004; Solomon & I. P. on Climate Change, 2007). Concerning the radiative effect of clouds and (global) precipitation, the cloud phase (water or ice) is one of the determining parameters (Boucher et al., 2013; Lau & Wu, 2003; Matus & L'Ecuyer, 2017; Mülmenstädt et al., 2015). Unfortunately, to date, clouds remain one of the largest uncertainties in climate models (Flato et al., 2014), with the cloud phase being especially challenging and varying from model to model (McCoy et al., 2016; Storelvmo et al., 2011; Waliser et al., 2009). Most models have rather too many liquid clouds or glaciate clouds too efficiently, that is, they have too many ice clouds (e.g., Cesana et al., 2015; Kay et al., 2016; Tan et al., 2025). This implies that the regime where mixed-phase clouds exist is often underrepresented. This regime can be characterized by the

supercooled liquid fraction (*SLF*)—the fraction of water that is present in clouds below 0°C, which is often used to characterize mixed-phase clouds. The estimation of the cloud phase is so complex because the phase change in clouds happens due to an interplay of many different processes and factors, some of which operate on a microscopic scale (e.g., Barrett et al., 2017a, 2017b; Tan & Storelvmo, 2016). The failed representation of clouds and cloud phase leads to an overestimation of the cloud climate feedbacks (Hofer et al., 2024; Li & Le Treut, 1992; Tan et al., 2016; Terai et al., 2016), which can lead to different climate responses to a doubling of CO_2 (climate sensitivity) between models (Dufresne & Bony, 2008; Zelinka et al., 2020). To understand and project changes in the climate system, it is therefore crucial to accurately represent cloud processes in models (Arakawa, 1975, 2004; Bony et al., 2006; Cess et al., 1989). In this study, we will focus on the different (microphysical) processes that influence the cloud phase by triggering the phase change of supercooled mixed-phase clouds. The focus is on the role of these processes and their importance within the overall context of the model's stratiform cloud microphysics, rather than on the specific parameterization schemes. The motivation is to highlight which processes and interactions can be interesting for further studies and improvement.

The phase change from liquid to ice (above −38°C), that is, the formation of mixed-phase or warm ice clouds, is triggered by different processes forming or introducing ice crystals in a supercooled cloud or supercooled cloud layer (thus reducing the supercooled liquid fraction):

1. *Heterogeneous freezing of supercooled cloud droplets in mixed-phase clouds*
   Supercooled cloud droplets can exist at temperatures as low as −38°C. At this temperature, all cloud droplets freeze to ice crystals homogeneously (this is a simplification, but a fair assumption which is commonly used in models). However, in the mixed-phase temperature regime above the homogeneous freezing limit, aerosols are needed to initiate the freezing (if no ice phase is present). The freezing temperature depends on the aerosol size and type, and the time the aerosol is exposed to a certain condition. Freezing is an important aspect of aerosol-cloud interactions. Extensive research has been done in the last decades investigating the role of different aerosols and their climate impact via the heterogeneous freezing pathway (e.g., DeMott et al., 2010; Hoose & Möhler, 2012; Kanji et al., 2017).
2. *Sedimentation of ice crystals from above*
   Ice crystals can fall from higher cloud layers or higher clouds into supercooled cloud layers, and supercooled clouds, respectively, due to gravity. One can distinguish between two cases: the seeder-feeder process versus in-cloud seeding. The seeder-feeder process entails long-lived ice crystals that fall from cirrus clouds (Braham & Spyers-Duran, 1967) or moist layers saturated with respect to ice (Bigg & Meade, 1970). Ice crystals that fall from upper cloud layers, often in cloud systems with high vertical extension, such as convective or frontal systems, are comprehended as in-cloud seeding. Several studies have investigated the occurrence of seeder-feeder situations in recent years (e.g., Di & Yuan, 2024; He et al., 2022; Proske et al., 2021; Ramelli et al., 2021; Vassel et al., 2019).
3. *Vertical transport of ice crystals*
   Ice crystals are transported not only via sedimentation due to gravity but also due to large-scale vertical advection and vertical diffusion (dynamical transport), which can lead to the introduction of ice crystals into supercooled clouds or supercooled cloud layers.
4. *Collision processes*
   Collision processes of hydrometeors involving ice-phase hydrometeors (liquid-ice or ice-ice collisions) can lead to an enhancement of ice particle numbers in case ice is introduced into the supercooled layer by one of the three aforementioned processes (Korolev & Leisner, 2020). This enhancement due to for example, the break-up of ice or droplet shattering, is called secondary ice formation.

In this study, we focus on the formation or introduction of ice crystals into supercooled clouds or supercooled cloud layers as the starting point of the possible phase transition of the cloud until full glaciation. This includes the aforementioned processes heterogeneous freezing of supercooled cloud droplets, sedimentation of ice crystals and vertical transport of ice crystals. These processes for triggering the phase change of the cloud are number-related, that is, creating or introducing an ice crystal, equivalent to changing the ice crystal number concentration. These processes also change the mass of the cloud ice inside the cloud, which is relevant for the final phase of the cloud but less for the initial triggering.

After the formation or introduction of the first ice crystals, other processes can take place and influence the delicate balance of supercooled water and ice in these clouds. These are (a) the Wegener-Bergeron-Findeisen

process increasing the ice mass due to the difference in saturation vapor pressure above ice and liquid water, (b) precipitation formation after the ice crystals reached a critical size, and (c) other microphysical processes, such as parameterized detrainment of ice crystals of convective clouds which increase the ice number and mass. However, in this study, we focus on the triggering of the phase transition for clouds in the mixed-phase temperature regime (between 0 and −35°C), not the phase development over time. Therefore, all processes that only change the cloud ice mass or increase existing ice crystal number concentration are not considered in this analysis.

Our study aims to analyze which process dominates the phase transition of stratiform mixed-phase clouds in ECHAM6.1-HAM2.3. This is important for understanding the complexity of microphysical parameterizations in a modeling framework and will guide further investigations to improve the representation of clouds and the respective cloud feedback.

2. Methodology and Overview of Simulations

For the sensitivity study of the importance of the ice-triggering processes presented here, we use the global climate model ECHAM6.1-HAM2.3 with a detailed two-moment microphysics scheme for stratiform clouds (Lohmann & Hoose, 2009; Lohmann et al., 2007; Neubauer et al., 2019; Zhang et al., 2012). Shallow and deep convective clouds are not using the two-moment microphysics scheme and are therefore not included in the analysis. More details about the relationship between the different cloud schemes can be found in Appendix A1.

Two of the ice-triggering processes, heterogeneous freezing and sedimentation of ice crystals, are described in the two-moment microphysics scheme. Heterogeneous freezing is parameterized aerosol-aware using dust (montmorillonite as a standard, assuming that all dust particles act as montmorillonite for freezing) for immersion and contact freezing and black carbon for immersion freezing (Hoose et al., 2008; Lohmann & Diehl, 2006). It is described by a deterministic scheme dependent on aerosol number (of the specific type) and temperature. This reference setup has a low onset freezing temperature (the temperature at which the freezing parameterization can freeze a significant number of cloud droplets, usually defined as 10%) and might be limited in terms of sources of ice-nucleating particles and in representing the natural mixture of dust types. More details on the freezing parameterization scheme can be found in Appendix A2.

The sedimentation of ice crystals is dependent on the size of the ice crystals and the thermodynamic conditions (temperature, pressure, and height) (Spichtinger & Gierens, 2009). The third ice-triggering process, vertical transport of ice crystals, is happening outside of the two-moment microphysics scheme. Instead, it is the dynamic scheme that can transport ice crystals vertically as a consequence of atmospheric motion. This movement of ice crystals can be upward or downward, the latter playing a larger role in ice cloud microphysics and in influencing the *SLF*. Processes that transport ice crystals vertically, and which are considered here, are large-scale vertical advection and turbulent mixing expressed via vertical diffusion. More details on sedimentation and the vertical transport of ice can be found in Appendix A3. Another important detail in the two-moment microphysics scheme of ECHAM6.1-HAM2.3 is the ice cloud threshold. All clouds, or rather cloud droplets, at a temperature ≤ -35°C are converted to the ice-phase.

The simulations were done for 1 year (2000) nudged to ERA-Interim reanalysis data with a resolution of T63 L31 (≈210 km horizontal resolution at the equator). We used nudging to reduce meteorological variability between the simulations in terms of dynamics (nudged variables: surface pressure, divergence, and vorticity) and to avoid the influence of possible temperature biases on ice formation (nudged variable: temperature). All simulations have the same set of tuning parameters, that is, no re-tuning was done for the respective other simulations to enable comparison of the simulations.

The simulations were analyzed by comparing the ice water content (*IWC*), liquid water content (*LWC*), and the *SLF* in mixed-phase clouds and by using the factorial method applied to *SLF*. *SLF* is defined as the ratio of cloud liquid water to all cloud water (liquid and ice) at a certain temperature. We used this quantity because it is specific to the mixed-phase cloud regime and is often used in other studies (e.g., Tan et al., 2016). However, one should bear in mind that *SLF* is based on the ratio of in-cloud ice and liquid water masses and not the number of cloud droplets and ice crystals, which is the quantity directly altered by the ice-triggering. Since the ice mass is changing as a consequence, we do not see this as a limitation of the analysis.

For this diagnostic, *SLF* for a certain temperature was calculated if this temperature exists within one cloudy model level (within the upper and lower bounds of a cloudy model level). In ECHAM6.1-HAM2.3, each model

Table 1
Overview of All Simulations (Ice-Triggering Process Is Switched On (YES, Abbreviated With Y) or Off (NO, Abbreviated With N) in the Respective Simulation)

Name of simulation	Mixed-phase cloud freezing	Vertical transport	Sedimentation
Standard (*Std*)	Y	Y	Y
No mixed-phase clouds (*No MPC*)	N	N	N
No mixed-phase cloud freez (*No freez*)	N	Y	Y
Only mixed-phase cloud freez (*Only freez*)	Y	N	N
No vertical transport (*No vtrans*)	Y	N	Y
Only vertical transport (*Only vtrans*)	N	Y	N
No sedimentation (*No sed*)	Y	Y	N
Only sedimentation (*Only sed*)	N	N	Y

level has a thickness in the vertical direction, defined by its upper and lower pressure (or height) boundaries. Physical quantities such as temperature and cloud water content are defined at the model mid-levels and stored as single values per model level, representing grid-box means (sub-grid variability of temperature and cloud liquid water is not resolved). To determine whether a model level contributes to the *SLF* at a given temperature T_{SLF}, we identify the model level whose vertical layer contains that temperature—that is, where the T_{SLF} lies between the upper and lower layer boundary temperatures. Temperatures at the layer boundaries are not prognostic variables, but are diagnostically obtained by interpolation between adjacent mid-level temperatures. These interpolated boundary temperatures are then used to determine whether a given temperature lies within a model layer. For example, if the upper bound of the model level has a temperature of −32°C and the lower bound temperature is −28°C, the cloud water values would be used to calculate the *SLF*(−30°C) since this temperature falls within this model level.

For the analysis, we used the 2k factorial experiment, or so-called factorial method (Kraut, 2015; Montgomery, 2013; Teller & Levin, 2008). This method can be used to estimate the impact of various conditions on the outcome of an experiment. In our case, the outcome of the experiment is the simulated *SLF* at a certain temperature, while the conditions are the (active or inactive) ice-triggering processes that can initiate the water-ice phase transition of a mixed-phase cloud and thus determine the cloud's *SLF*. The conditions consist of three factors (controlled parameters), the three different ice-triggering processes: heterogeneous freezing in mixed-phase clouds (*freez*), sedimentation of ice crystals (*sed*), and vertical transport (vertical diffusion and vertical advection of ice crystals; *vtrans*). These factors can depend on or interact with each other. Each factor (ice-triggering process) can be switched on or off in the simulation setup, that is, each factor has two possible values, so-called levels. The number of factors (3) and the number of levels (2) result in a total number of possible combinations of factors and levels of $2^3 = 8$, meaning that for the method, eight simulations were done to identify the contribution of each process to *SLF* at different temperatures. The eight simulations reflect all combinations of ice-triggering processes being active or inactive. The overview of all simulations and the corresponding abbreviations can be found in Table 1.

The simulated *SLF* (global annual mean value for each simulation) is used to calculate the effect of each factor, that is, the change of the simulation result (which is the simulated *SLF*) depending on the level (ice-triggering process switched on or off). The effect of each factor can also be expressed as the average sensitivity of the simulation result to a change in a factor, that is, an ice-triggering process on/off. It is estimated by subtracting the average of the simulated *SLF* when the ice-triggering process is switched off from the average of the simulated *SLF* when the ice-triggering process is switched on. To give a concrete example, the effect of freezing on *SLF* in our simulation setup is calculated as follows:

$$Eff_{freez} = \frac{1}{4}\cdot\left(SLF_{Only\ freez} + SLF_{No\ vtrans} + SLF_{No\ sed} + SLF_{Std}\right) - \frac{1}{4}\cdot\left(SLF_{No\ freez} + SLF_{Only\ vtrans} + SLF_{Only\ sed} + SLF_{No\ MPC}\right) \quad (1)$$

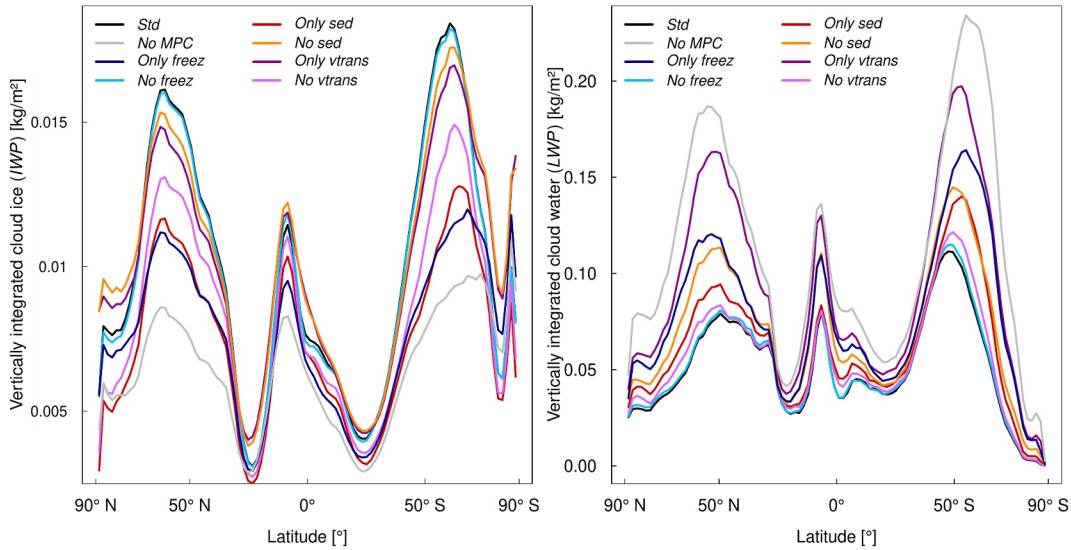

Figure 1. Annual zonal mean of vertically integrated cloud ice (cloud ice water path, *IWP*) and vertically integrated cloud water (cloud liquid water path, *LWP*) for the eight different simulations (see Table 1). *IWP* and *LWP* are derived over the whole atmospheric column and thus include all cloud types. Additionally, *IWP* and *LWP* count only in-cloud hydrometeors and therefore exclude precipitating hydrometeors, but are counted over all vertical levels.

The consideration of the interaction of the factors is taken care of due to the experimental design (all possible combinations are simulated).

As highlighted by Teller and Levin (2008), the factorial method has the advantage over the often used factor method (e.g., Stein & Alpert, 1993) that the relative contribution of a factor of all possible interactions is estimated and not only the relative contribution of each factor (ignoring all possible interactions). Another advantage of this method is that it is computationally cheap if the number of factors and levels is not too large, and it is easy to use. Moreover, the biggest advantage compared to other techniques, such as using emulators, is that the same framework can be used on the output of different models, enabling the comparison of the same sensitivity test over a range of models.

3. Results

In this section, we start with an overview of the cloud ice and cloud water and the role of the ice-triggering processes for the integrated cloud ice, cloud water, and respective super-cooled liquid fraction, followed by the statistical analysis. Figure 1 shows an overview of the annual zonal mean vertically integrated cloud water and cloud ice for all eight simulations. The respective global annual mean values are presented in Appendix B (Table B1). This Figure represents the total cloud ice and cloud water including all cloud types (warm clouds, mixed-phase clouds and cirrus clouds). As shown in previous studies (Neubauer et al., 2019) and compared to other simulations (e.g., Eriksson et al., 2026), all simulations show a typical zonal variation in cloud water and ice. The ice water path (*IWP*) is on the low end of the spectrum—this underestimation is very likely due to missing precipitating hydrometeors that are neglected when calculating *IWP*.

In Figure 1, the specific simulations can be compared relative to the *Std* simulation (black line; including all ice-triggering processes in the mixed-phase cloud regime) and the *No MPC* simulation (gray line; excluding all processes triggering ice in the mixed-phase cloud regime), where no mixed-phase clouds are formed (instead, liquid or ice clouds do form). The *Std* simulation has the lowest/highest vertically integrated cloud water/cloud ice (liquid water path (*LWP*): 55.81 g m^{-2}; *IWP*: 9.18 g m^{-2}), while the *No MPC* simulation has the lowest/highest vertically integrated cloud ice/cloud water (*LWP*: 109.76 g m^{-2}; *IWP*: 5.96 g m^{-2}), respectively. Comparing these two simulations show that a large part of the total ice is due to cirrus effects. This is a limitation when analyzing the specific simulations regarding their role for the mixed-phase regime ice using Figure 1.

We can still derive some first findings on the ice-triggering processes: it can be seen in Figure 1 that the *IWP* of *Only freez* is the second lowest after *No MPC*, and thus we conclude that freezing is the process triggering the smallest amount of ice in mixed-phase clouds (at least in the absence of other triggering processes). Nearly identical cloud ice as in the *Std* simulation is triggered in the simulations without freezing (*No freez*) and the ones with vertical transport (*Only vtrans*, *No sed*). Accounting for two of the three ice-triggering processes triggers more ice formation than accounting for one single process (except for vertical transport; *Only vtrans*).

The implication for the cloud liquid water by the different ice-triggering processes is similar, but some differences exist. The cloud liquid water is highest and thus most similar to the *No MPC* simulation in simulation *Only vtrans*. A higher amount of cloud liquid water compared to the *Std* simulation can be seen in the simulation *Only freez*, where the high cloud liquid water could be related to the reduced transformation of cloud water to cloud ice (cloud ice closest to the *No MPC* setup). Of all sensitivity simulations, the cloud liquid water of the ones that include sedimentation (simulations *No freez*, *No vtrans*, *Only sed*) are closest to the *Std* simulation (and furthest away from the *No MPC* simulation). Besides, the simulation with only sedimentation (*Only sed*) is the one simulation with only one process that is closest to the *Std* simulation. This highlights the role of sedimentation for precipitation/snow formation, thus reducing the total cloud water.

To confirm our findings and overcome the limitation of comparing vertically integrated quantities including all cloud types, it is helpful to look at the vertical distribution as well. Figure 2 expands on Figure 1 by showing the vertical distribution of ice and liquid water (ice water content (*IWC*) and liquid water content (*LWC*)) for all simulations. Note that even here, all clouds are included. We can split up the simulations into two sets, indicated in Figure 2 by the two columns for *IWC* and *LWC*. The left column shows the *Std* simulation and the three simulations that look very similar to it in terms of the *IWC*, respectively *LWC*, pattern (the simulation closest to *Std* is *No freez* for *IWC* and *LWC*), and the right column shows the simulation without mixed-phase clouds (*No MPC*) as well as the three simulations most similar to *No MPC* (the simulation closest to *No MPC* is *Only freez* for *IWC* and *LWC*). When comparing the two sets, for *IWC*, one difference is noticeable: the *IWC* is spread throughout the entire vertical depth of the mixed phase cloud regime in the left plots, while in the right plots, the *IWC* is mostly present in the cirrus regime and limited to higher levels of the mixed phase cloud regime. As a comparison, the simulation *No MPC* shows only ice in the cirrus regime. Note that the *IWC* is higher in the cirrus regime in the *No MPC* simulation compared to the *Std* simulation, despite nothing being changed in the setup considering the cirrus ice formation. This is due to the missing sedimentation that transports the ice crystals formed in the cirrus regime to lower levels into the mixed-phase regime. The simulation *No MPC* shows clearly that one of the processes (sedimentation, freezing, or vertical transport) is needed to form or transport ice crystals in the mixed-phase cloud regime. The simulation *Only freez* shows that freezing seems to trigger ice but only within the lower temperatures, that is, upper levels of the mixed-phase cloud regime. This can be explained by the low freezing efficiency of montmorillonite, which is the aerosol type used in the reference setup of ECHAM6.1-HAM2.3. This reference setup for freezing is likely an underestimation of the true nature, where a mix of dust types (including more efficient dusts than montmorillonite) and other aerosol types, for example, bioaerosols, are present (Kanji et al., 2017). Having vertical transport switched on (simulation *No sed* and *Only vtrans*) spreads the cloud ice throughout the mixed-phase regime, but not as strongly as compared to simulations with sedimentation switched on (left column). Sedimentation and vertical transport together (simulation *No freez*) result in a qualitatively similar *IWC* as in the *Std* simulation regarding the pattern. The height information helps us to understand Figure 1. For example, the *IWP* of simulation *No sed* was very close to the *Std* in Figure 1, but Figure 2 shows that this is likely due to a large contribution of cirrus clouds to the *IWC* (since ice crystals cannot sediment), so not so much related to a realistic representation of the mixed-phase. The same is true for simulation *Only vtrans*, where the sedimentation is missing to remove ice from the cirrus regime.

When comparing the two columns in Figure 2 for *LWC*, a similar pattern is visible: the liquid water has a higher vertical extent, that is, reaching up to higher altitudes for the trio of simulations that are most alike *No MPC* (*Only freez*, *No sed* and *Only vtrans*; right column). Here, the ice production is suppressed, and therefore, supercooled liquid water exists throughout the whole mixed-phase regime.

Summarized, we can state that Figures 1 and 2 imply that heterogeneous freezing is not the dominant process triggering ice in the mixed-phase cloud regime. Instead, sedimentation plays a crucial role. However, no single process alone is enough for good performance—a combination of at least two of the three ice-triggering processes is needed to get the same amount of cloud ice in the mixed-phase regime as in the *Std* simulation. With

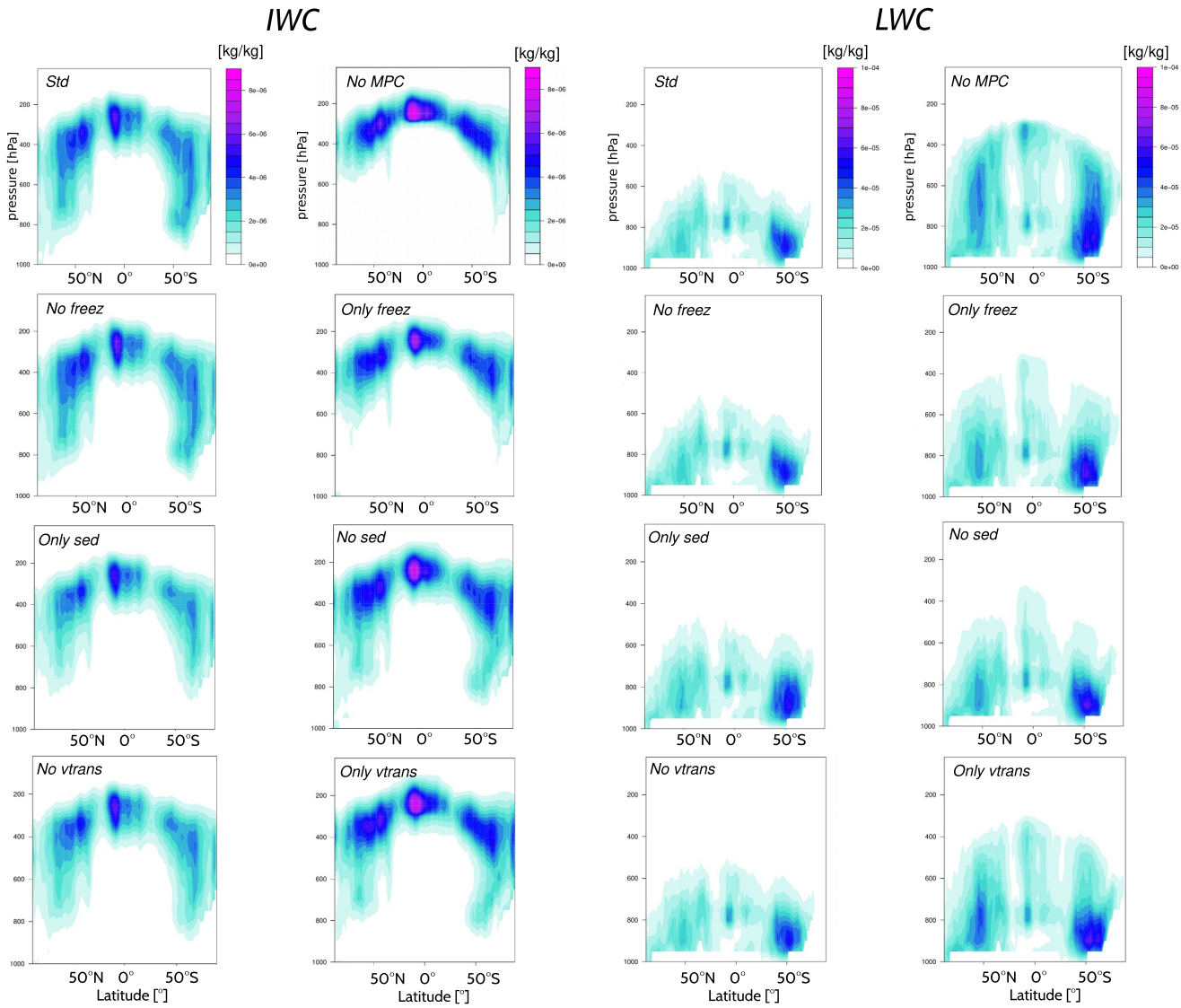

Figure 2. Annual height-resolved zonal mean of ice water content (*IWC*) and liquid water content (*LWC*) for the eight different simulations (see Table 1). Left column: *Std* simulation and the three simulations most alike *Std* in terms of the *IWC* pattern (closest to *Std* is *No freez*); right column: simulation without mixed-phase clouds (*No MPC*) and the three simulations most alike *No MPC* (closest to *No MPC* is *Only freez*).

sedimentation or vertical transport turned off, freezing can improve the simulation. These findings are consistent with previous results from Dietlicher et al. (2019).

Both *IWP* and *LWP* are not purely determined by mixed-phase clouds, but also by cirrus and warm clouds (if not limited by levels or temperatures that are specific to mixed-phase clouds). We therefore calculated a variable that is unique for the mixed-phase cloud regime, which is the supercooled liquid fraction within a cloud (*SLF*) (e.g., Tan et al., 2016). The same variable is used for the analysis using the factorial method in Section 3.1.

Figure 3 shows the results of the estimated annual global mean *SLF* at different temperatures for all simulations. The corresponding values can be found in Appendix C (Table C1). The simulation *No MPC*, where all ice-triggering processes are switched off, contains only liquid clouds in the mixed-phase temperature regime. The *No MPC* simulation can therefore be seen as one extreme for *SLF*. In this case, *SLF* is expected to be one at all temperatures until −35°C (no ice is triggered). At −35°C, one would expect an *SLF* of zero in the *No MPC* simulation since all supercooled water is transferred to ice at this temperature (cloud ice threshold). The *SLF* is not exactly zero here due to the methodology of the diagnostics. As described in Section 2, a model level with lower/

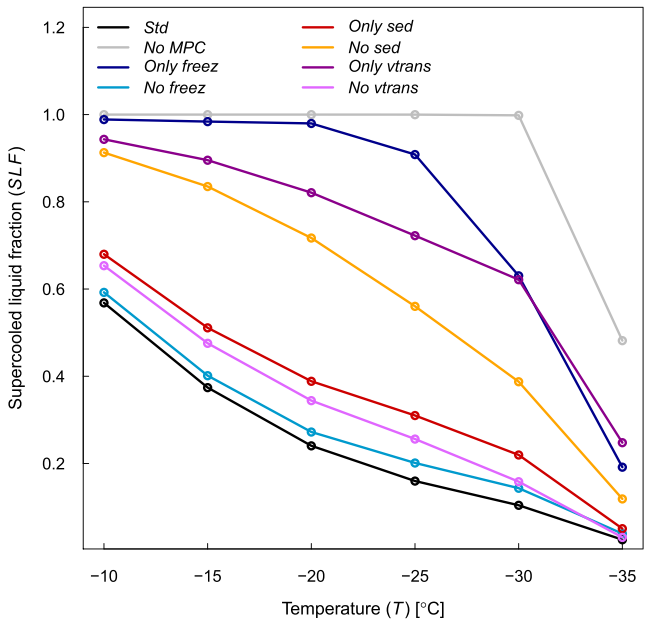

Figure 3. Global annual averaged supercooled liquid fraction (*SLF*) at different temperatures for all simulations. The analogous figure for thin clouds and cloud tops ($\tau < 3$) can be found in Appendix D (Figure D1).

higher temperature bounds below/above −35°C would be used for the *SLF* calculation at −35°C. However, for the parameterizations of cirrus and mixed-phase clouds, the mean temperature of the model level is used, for example, a mean temperature of −36°C would mean to be in the cirrus regime, a mean temperature of −34°C would mean to be in the mixed-phase cloud regime instead. This implies that the diagnosed *SLF* at −35°C consists of cloud water and ice values both from the cirrus and the mixed-phase cloud regime (mean temperature can be below −35°C, i.e., in the cirrus regime). The reason is the coarse vertical resolution, which entails that the model levels have such a wide temperature range that they can be attributed to different cloud regimes.

While the *No MPC* simulation can be seen as one extreme for *SLF* (highest *SLF*), the *Std* simulation will result in the lowest *SLF* values (all ice-triggering processes switched on). In the following, we compare the simulations to these two extremes (*No MPC* and *Std*). The *SLF* estimate of the simulations *Only freez* and *No freez* can give some further indication of the role of freezing as a trigger process for the mixed-phase. Freezing alone hardly leads to any ice in mixed-phase clouds (*SLF* very close to *No MPC* estimate) until a temperature of −25°C. Below that, its importance increases. This is probably caused by the freezing parameterization scheme with a low onset freezing temperature. This is consistent with the interpretation of Figures 1 and 2. Another interesting finding that can be confirmed by Figure 3 is that simulations with only one trigger process active mostly result in higher *SLF* values, that is, less triggered ice, than all other simulations. The only exception is the simulation *Only sed*—this simulation is similar to the *Std* simulation, while the simulation without sedimentation (*No sed*) results in similarly high *SLF* as the other simulations with only one trigger process. This highlights the role of sedimentation in triggering ice in mixed-phase clouds.

An aspect, which can be seen in Figure 3, the *SLF* diagram, is how the *SLF* is changing with temperature, that is, how strongly specific ice-triggering processes, or a combination of several, depend on temperature. The decrease of *SLF* with temperature can be described as close to linear (sigmoidal), as can be seen in satellite retrieval data (e.g., Bruno et al., 2021; Komurcu et al., 2014; McCoy et al., 2016). The temperature dependence of *SLF* in the *Std* simulation follows a similar linear decrease. In contrast to that is the temperature dependence of the *Only freez* simulation, which is highly non-linear as a result of the freezing parameterization and the onset freezing temperature of montmorillonite at low temperatures. For some processes, it can be seen that the temperature dependence changes with decreasing temperature, leading to a non-linearity. For example, for the vertical transport (*Only vtrans*), *SLF(T)* is close to linear until a temperature of −30°C and changes afterward. This can be attributed to a change in the importance of freezing and vertical transport (the lines cross in Figure 3, which is even more explicit in Figure 4 in the next section).

Summarizing the analysis, freezing alone is not important for triggering ice at warm mixed-phase temperatures until −25°C. It can lead to ice in mixed-phase clouds when combined with other ice-triggering processes such as vertical transport or sedimentation, which likely transport the ice crystals formed at colder parts of the cloud (sufficiently cold for freezing to occur) into warmer regions. However, sedimentation is the most important single process, and combined with vertical transport, it reproduces a very similar qualitative picture as the *Std* of ECHAM6.1-HAM2.3.

3.1. Results Using the Factorial Method

As described in the methods section (Section 2), we used the factorial method with *SLF* as the variable to analyze and quantify the importance of the three ice-triggering processes. The calculated contribution (effect) to *SLF* for each ice-triggering process based on Equation 1 can be seen in Figure 4. The difference compared to Figure 3 is that the factorial method includes all processes when calculating the cumulative effects, which means that instead of comparing specific simulations, for example, *No Sed* versus *Only sed*, the total contribution of each process can be compared, taking the interactions between the processes into account, for example, the total role of

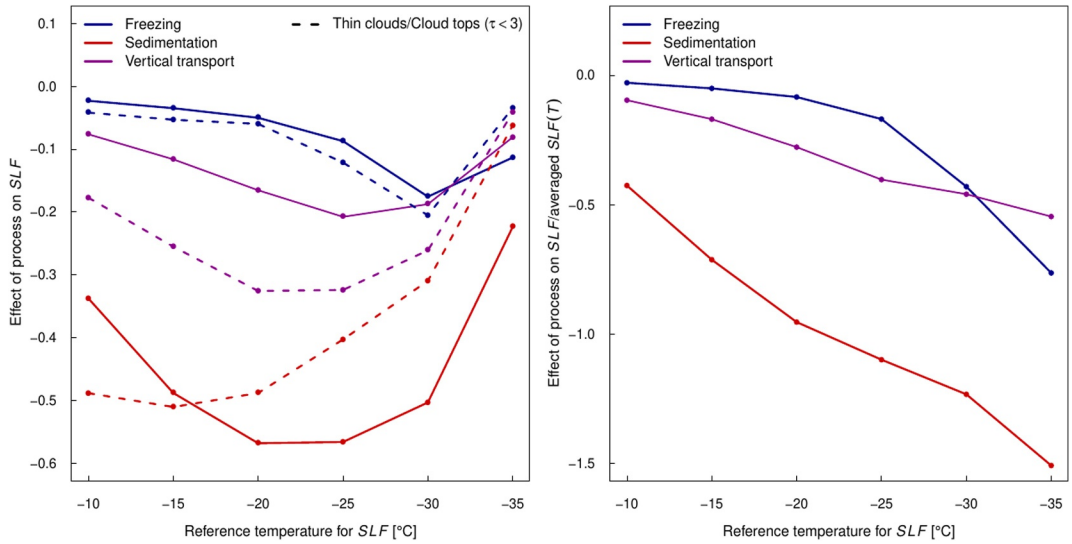

Figure 4. Quantitative contribution of each triggering process to the estimated *SLF* calculated using the factorial method. The solid line shows the estimate of the quantitative contribution as explained above; the dashed line is the same analysis restricted to thin clouds and cloud tops with $\tau < 3$ (see Section 3.2). The figure in the right panel shows the normalized effect by the averaged SLF over all simulations for each temperature.

sedimentation for *SLF* based on all simulations. As shown in Figure 4, the effects of all three factors are negative, that is, the process decreases the *SLF*. In this case, if the strength of a triggering process is increased, *SLF* decreases. A relatively strong trigger process leads to more ice in mixed-phase clouds, thereby reducing the amount of supercooled water and, consequently, *SLF*. Since *SLF* decreases with temperature, that is, the cloud is glaciating, the sum of the quantitative contribution of all the ice-triggering processes is not constant with temperature. Instead, the sum of the quantitative contribution of all the ice-triggering processes is more negative the lower the temperature (until −30°C), which reflects that together all ice-triggering processes are stronger with decreasing temperature, leading to a reduction of *SLF*. The temperature behavior of each line (for each process) in Figure 4 is thus determined by two factors: the relative role of the processes with respect to the others and the general increase of the effect of all processes on SLF with decreasing temperature. To understand the temperature behavior of the effect of all processes better, we added a normalized figure in Figure 4 (right panel). The effect of each process is here normalized by the average SLF over all simulations, that is, representing the fraction of how many clouds glaciated at this temperature.

Note that for the −35°C bin the SLF is underestimated because of the sharp transition to cirrus clouds in the model and the coarse resolution, leading to cloud water and ice values both from the cirrus and the mixed-phase cloud regime in this temperature bin. That leads to a bias in the estimated effect at this temperature as well.

The analysis shown in Figure 4 confirms the preceding results, adding more detail:

1. All the triggering processes have a non-linear influence on *SLF* in dependence on *T*. The non-linearity disappears when taking all processes into account (despite the jump in *SLF* at −35°C, which is due to the internal sharp transition to cirrus clouds in the model). The non-linearity can partially be attributed to the interaction of the processes. For example, for the vertical transport, *SLF(T)* is close to linear until a temperature of −30°C and changes afterward. This can be attributed to a change in the importance of freezing and vertical transport (the lines cross in Figure 4). Looking at the normalized version of the effects, it can be seen that all processes show a stronger effect the colder the temperature. This clearly shows that the effect of all processes strongly depends on temperature, either because the process itself is strongly temperature dependent (e.g., freezing) or because the process is strongly dependent on the other processes that are temperature dependent (which may explain the behavior for sedimentation). Note that the concrete values shown in the normalized Figure are not meaningful since averaging the SLF over all simulations does not give any physically meaningful value, and the bounds of SLF (between 0 and 1) can create a bias.

2. Sedimentation is crucial for the mixed-phase clouds in ECHAM6.1-HAM2.3. Sedimentation has a larger role compared to freezing across the whole temperature range, with the largest influence in the temperature range between −20°C and −25°C. Below −25°C, the role of sedimentation decreases, but it remains the most important process. Vertical transport is the second important triggering process with a similar behavior to sedimentation. However, both processes only play a role if ice exists that can be sedimented or transported vertically. That means that non-local processes are governing the *SLF* in mixed-phase clouds.
3. Heterogeneous freezing rarely seems to trigger ice at temperatures above −25°C. At temperatures colder than −30°C, freezing becomes more important than vertical transport, and the role of sedimentation is less pronounced. The same was found in Dietlicher et al. (2019), which indicates that the factorial method can be used as a sufficient and easy complementary approach to investigate the contribution of ice-trigger processes (or similar).

3.2. Sensitivity Test: All Clouds Versus Thin Clouds and Cloud Tops

In the preceding analysis, we showed that sedimentation and the transport of ice crystals are crucial for the magnitude of *SLF* in mixed-phase clouds. To distinguish between different cases of seeding, we examined whether the vertical dimension of the cloud plays a key role in ice-triggering. Therefore, we did a sensitivity test for clouds filtered by cloud optical depth. Specifically, counting from the cloud top, we counted until the lowest layer for which the summed cloud optical depth (τ) of all the above layers remained smaller than three. This represents thin clouds ($\tau < 3$ in total) and deeper cloud tops (the topmost cloud layers until a τ of 3) (Min et al., 2004; Wang & Min, 2008). Note that optical depth is only an approximate indicator of vertical cloud extent, and it would be more correct to use physical cloud depth instead. However, ECHAM6.1-HAM2.3 assumes a cloudy model level (as estimated via the horizontal cloud fraction) to be cloudy throughout the entire layer. Because the model does not represent vertical variability of cloud fraction within a layer, deriving a meaningful geometric cloud thickness would require additional assumptions about the vertical distribution of cloud. For the presented sensitivity test, cloud optical depth provides a straightforward and internally consistent way to distinguish optically thin cloud tops (where seeding is limited) from optically thicker clouds (where sedimentation is more active).

The quantitative contribution of each ice-triggering process to the estimated *SLF* in thin clouds and cloud tops as compared to all clouds can be seen as the dashed lines versus solid lines (all clouds) in Figures 3 and 4. For heterogeneous freezing, there is hardly a difference between the two cases, which is expected since this process is purely temperature dependent (the vertical structure of the cloud is not important). For sedimentation, however, the contribution as a trigger process is substantially reduced in thin clouds and cloud tops. This indicates that extensive in-cloud seeding in thick clouds occurs in the all-clouds setup. In thick clouds, ice particles can sediment from upper (colder) to lower (warmer) levels, where the temperature is too warm to initiate heterogeneous freezing. In-cloud seeding, that is, sedimentation of ice crystals from colder cloud layers, reduces both the supercooled water and *SLF*. Thus, sedimentation in thick clouds plays a crucial role as a triggering process. This effect is reduced in thin clouds and cloud tops, where the sedimentation of ice particles within the clouds from higher to lower levels has less of an impact because the temperature does not differ much between the upper and lower bounds of the thin clouds or the cloud top layer. The temperature dependence of the contribution of sedimentation changes for the two cases. In the standard setup of the model (*Std*), sedimentation is most important in the temperature range from −20°C until freezing becomes efficient. For thin clouds and cloud tops, sedimentation is most important at −10°C but loses importance with decreasing temperature. Vertical transport, that is, vertical diffusion or vertical advection, is relatively more critical for thin clouds and cloud tops compared to all clouds. A concluding result is that especially thick clouds are essential to enable sedimentation and transport to play a major role in ice-triggering, and as such for the cloud phase for mixed-phase clouds in ECHAM6.1-HAM2.3 (as has been shown as well by Dietlicher et al. (2019)).

4. Discussion and Conclusions

In this study, we investigated the role of three ice-triggering processes for the phase of clouds in the mixed-phase temperature regime (between 0 and −35°C) in the global climate model ECHAM6.1-HAM2.3. The three investigated ice-triggering processes, which can lead to the initial formation of ice crystals in a supercooled cloud, are heterogeneous freezing, sedimentation of ice crystals from upper cloud layers (in-cloud seeding and seeder-feeder process), and vertical transport (vertical diffusion and vertical advection) of ice crystals. For the analysis,

an ensemble of simulations was realized, and the supercooled liquid fraction (*SLF*) of mixed-phase clouds was used as an indicator of the cloud's microphysical structure and phase. The simulation results were analyzed utilizing a statistical framework, specifically the factorial method.

The analysis shows that at least two of the three ice-triggering processes are needed to get the same amount of cloud ice in the mixed-phase regime compared to the standard setup of the model (*Std*). However, it is evident that the sedimentation of ice crystals and the vertical transport of ice crystals are crucial for triggering ice in mixed-phase clouds in ECHAM6.1-HAM2.3 and shape the magnitude of *SLF* as has been shown previously by Dietlicher et al. (2019). Sedimentation is the most important single process with the largest influence in the temperature range between −20°C and −25°C. Vertical transport, the second important ice-triggering process, and sedimentation are limited by the fact that ice needs to exist to be transported vertically. The dominance of sedimentation and vertical transport raises the question of the context and cloud types, where ice-triggering occurs. The analysis was therefore complemented by a sensitivity test on cloud (tops) with an optical thickness smaller than three (i.e., thin clouds and the top of deeper clouds). This showed that especially thick clouds are essential to enable sedimentation and vertical transport to play a major role in ice-triggering. It is thus both a classical seeder-feeder situation (e.g., Bigg & Meade, 1970; Braham & Spyers-Duran, 1967), where ice crystals fall from cirrus clouds into supercooled clouds, and in-cloud seeding that is present in our simulations. Proske et al. (2021) showed that in-cloud seeding is more prevalent than the seeder-feeder process in the special case of seeding by cirrus cloud layers, which agrees with our findings. In-cloud seeding can occur in frontal or other clouds with a large vertical extent, where lower cloud levels are fed with ice crystals from higher and colder cloud levels, where freezing happens. In this context, it is important to discuss the model resolution. The existence of thick clouds can be a result of a coarse and thus insufficient model resolution, as in ECHAM6.1-HAM2.3 with model levels of several hundred meters. Sub-saturated cloud layers are not necessarily resolved so that falling ice crystals survive and seed the lower cloud layers they fall into. However, the poor vertical resolution can, on the other hand, suppress the classic seeder-feeder situation because the ice crystals need to survive a very long vertical distance without sublimating while falling through this subsaturated layer. It has been shown in other studies that vertical resolution is a limiting factor for getting the cloud phase correct in climate models (Barrett et al., 2017b), for different reasons. In conclusion, it is difficult to derive information from this study on how often and what kind of seeder-feeder situation happens and dominates the ice-triggering. Still, any movement of ice crystals in the vertical within a cloud (by sedimentation or vertical transport) seems to play a crucial role for the cloud phase. As an outlook, it would be interesting to repeat the analysis in a model setup with a different vertical resolution. It is of interest to mention that other studies also highlighted the importance of sedimentation compared to freezing (e.g., Tan & Barahona, 2022).

Regarding the role of sedimentation, in-cloud seeding, and the seeder-feeder process, it is worthwhile to draw our attention to the question of the realism of our findings. There is, however, only a limited number of studies examining this specific aspect (e.g., in recent years focusing on different regions: Achtert et al. (2026); Di and Yuan (2024); He et al. (2022); Proske et al. (2021); Ramelli et al. (2021); Vassel et al. (2019)), and it has not been conclusively assessed yet. One example of this non-conclusivity is the contradictory finding of three studies of Arctic clouds (note that cloud characteristics often differ substantially from those at lower latitudes and therefore may not be representative globally). de Boer et al. (2011) found little occurrence of multilayer clouds in the Arctic and argued that seeding is unlikely. In contrast to that, Achtert et al. (2026) and Vassel et al. (2019) report frequent occurrences of multilayer clouds and cases of cloud seeding.

Another major result of the study is the implication that heterogeneous freezing is not the dominant process triggering ice in the mixed-phase cloud regime. Heterogeneous freezing rarely seems to trigger ice in mixed-phase clouds in ECHAM6.1-HAM2.3 at temperatures above −25°C, which follows the used freezing conditions (parameterization scheme). Villanueva et al. (2021) shows a similar behavior for ECHAM-HAM-P3 and E3SM when looking at cloud ice frequency (their Figure 2c). However, freezing can lead to ice in mixed-phase clouds when combined with other ice-triggering processes, such as vertical transport or sedimentation, which can transport the newly frozen ice crystals from colder parts of the cloud into warmer regions. Below −25°C freezing plays a clear role as apparent in the factorial method. The strong contribution of vertical transport and sedimentation can hide a potential aerosol effect in models. Before too strong conclusions are derived when it comes to the sensitivity of the model to freezing parameterizations and variations in aerosol-cloud interactions, a few things should be noted here:

1. The analysis is based on the mean-state SLF. However, freezing likely controls the spatiotemporal variability of SLF, as shown in Villanueva et al. (2021). To investigate the spatiotemporal importance of the ice-triggering processes is beyond the scope of this study, but could be an interesting follow-up.
2. Our findings are true for the specific model version used in this study. Other model versions or other models could infer different results for the same analysis (see, e.g., Frostenberg et al. (2026)).
   As mentioned earlier, the findings might be highly dependent on the freezing parameterization scheme, which might underestimate the role of freezing due to the specific choice of ice-nucleating particles or missing sources of these. However, our findings do not necessarily have to be linked to a specific freezing parameterization, but likely also depend on other factors or parameterization schemes that are interlinked with the freezing scheme, for example, the sedimentation of ice crystals, the Wegener-Bergeron-Findeisen process, or the missing representation of secondary ice processes (SIP). SIP can mask signals when investigating cloud ice—for example, through enhanced sedimentation due to increased numbers of ice crystals. However, Proske et al. (2023) and Frostenberg et al. (2026) found that SIP is not dominant in ECHAM6.1-HAM2.3, so we do not expect a substantial impact of this missing aspect on our conclusions. Note that the SIP parameterizations used in these two studies included only the Hallett-Mossop process and a combination of Hallett-Mossop, ice-ice collisional break-up, and droplet-shattering, respectively. The conclusions likely depend on these parameterizations, but also on the host model, and need not imply that SIP is not important in reality.

   Thus, repeating the same analysis with different models could be of interest to consolidate our findings.

Interesting in this context is to mention other studies that partially promote the derived conclusions on the role of heterogeneous freezing. In the study of Komurcu et al. (2014), it is shown that *SLF* varies between models even when the same freezing parameterization scheme is used. This could be related to the weak role of the freezing parameterization compared to the other processes in the investigated models. When it comes to the question at which temperature the freezing gains more importance compared to the other processes, field studies by Ansmann et al. (2009) based on LiDAR observations show that glaciation occurs below −20°C likely by heterogeneous freezing and above that temperature the glaciation can be attributed to the seeder-feeder process.

A limitation of the analysis is that the analyzed variable (*SLF*) that was used (especially for the factorial method) is mass and not number-based, while the ice-triggering processes are the latter (even though they affect both number and mass). The ice-triggering processes lead to an initial concentration of ice crystals that grow in mass by the Wegener-Bergeron-Findeisen process, but the ice crystal number concentration and mass are also enhanced due to the detrainment of convective condensate when ice is present.

We should also stress that the results here stem from a "model world" analysis, which does not necessarily reflect experimental findings or our conceptual understanding. The discrepancy between modeled findings and conceptual understanding, that is, that heterogeneous freezing is important for the phase of mixed-phase clouds throughout a wide temperature regime, highlights how important this topic is for model development.

To gain more clarity on the ice-triggering process in nature and to facilitate model development, we highlight here the need for observational constraints of ice-triggering processes (ideally, process rates). Constraining state variables (*LWC*, *IWC*, *SLF*), as used in Carlsen and David (2022); Proske et al. (2021); Villanueva et al. (2021), is not sufficient as biases in processes can compensate each other. We acknowledge that process rates remain challenging to infer from observations, and base-state variables continue to be the most accessible constraints. This raises the question of how base-state variables can be used to constrain quantities such as *SLF* and thereby improve our understanding of ice-triggering processes. One potential approach is to derive observational constraints for distinct cloud and temperature regimes, thereby limiting the set of processes that can explain the observed ice. Furthermore, developing observational products tailored to model development for the ice phase would be highly valuable.

Finally, we would like to underline that the factorial method, as an easy-to-use statistical framework, did provide interesting and reasonable results compared to previous studies (Dietlicher et al., 2019) and is therefore an excellent tool to investigate the role of ice-trigger processes (or similar questions), especially for several models in comparison.

Appendix A: Additional Model Details of ECHAM6.1-HAM2.3 and the Two-Moment Cloud Microphysics Scheme

A1. Stratiform Versus Shallow and Deep Convective Clouds

In ECHAM6.1-HAM2.3, both the shallow and deep convection schemes use one-moment microphysics and therefore do not interact with the two-moment microphysics directly. However, when convective and stratiform clouds coexist in the same grid box, the model detrains condensate (cloud liquid water and/or cloud ice) from convection into the stratiform cloud field. This detrained condensate is incorporated into the stratiform cloud condensate budget (as ice if cloud ice is present within the mixed-phase temperature regime, as liquid otherwise). Additionally, the number concentrations of cloud droplets or ice crystals are also added for the detrained condensate; the procedure is described in Neubauer et al. (2019). Since detrained condensate does not trigger ice formation in mixed-phase clouds and only contributes to the mass and number concentrations within the existing stratiform cloud, the focus of this study is on stratiform clouds by model design.

A2. Parameterization of Freezing in Mixed-Phase Clouds

In ECHAM6.1-HAM2.3, contact and immersion freezing is described aerosol-aware and deterministic as a function of temperature and aerosol number in the cloudy grid-boxes, that is, where cloud liquid water is present. As ice-nucleating particles, the dust types montmorillonite and black carbon are used for immersion freezing, while dust (montmorillonite) is used for contact freezing (Hoose et al., 2008). Marine organic aerosols and bacteria have been implemented as potential ice nucleating particles in the past (Huang et al., 2018; Sesartic et al., 2012), but are not included in the standard version of the model because they are negligible compared to dust and therefore not used here.

Contact freezing is negligible compared to immersion freezing, and therefore we focus on immersion freezing only.

The freezing parameterization used for immersion freezing of dust (montmorillonite) and black carbon is an empirical parameterization scheme (Lohmann & Diehl, 2006) based on wind-tunnel studies summarized in Diehl and Wurzler (2004). Freezing is characterized by an exponential rate function J_{imm}, which is expressed as follows:

$$J_{\mathrm{imm}} = a \cdot N_{\mathrm{a,imm}} \cdot \exp(a \cdot (273.15\ \mathrm{K} - T)) \cdot \frac{dT}{dt} \cdot \frac{\rho_{\mathrm{air}} \cdot q_{\mathrm{l}}}{\rho_{\mathrm{l}}} \tag{A1}$$

with $N_{\mathrm{a,imm}}$ the number of immersion nuclei (i.e., the number of dust or black carbon particles that can initiate freezing, see below), T is the grid-box mean temperature, t the time, ρ_{air} the air density, ρ_{l} the density of the cloud droplet, q_{l} the cloud liquid water mass-mixing ratio in the cloud and $a = \mathrm{K}^{-1}$. The number of immersion nuclei $N_{\mathrm{a,imm}}$ is obtained from the number of aerosols in the aerosol modes of the M7 aerosol scheme in ECHAM6.1-HAM2.3 that potentially can initiate the freezing process (black carbon in the soluble mode and accumulation mode dust aerosols) multiplied by a temperature dependence of individual species x:

$$N_{\mathrm{a,imm}} = \sum_{x} c_x \frac{N_{\mathrm{imm},x}}{N_{\mathrm{aer,tot}}^{>35\ \mathrm{nm}}} = N_{\mathrm{a,imm,dust}} + N_{\mathrm{a,imm,black\ carbon}} \tag{A2}$$

where $N_{\mathrm{aer,tot}}^{>35\ \mathrm{nm}}$ is the total number of aerosol particles larger than 35 nm, c_x is a species specific empirical factor, which is 32.3 for montmorillonite and $2.91 \cdot 10^{-3}$ for black carbon. Note that in contrast to many other freezing schemes, for example, the active site density scheme or schemes based on Classical Nucleation Theory, the size of the particle is not relevant for the freezing rate.

A3. Parameterization of Sedimentation and Vertical Transport

Although sedimentation and vertical transport both describe vertical motion of ice crystals (sedimentation limited to downward motion) and thus contribute to processes such as the seeder-feeder process, they are separated mechanistically and parameterized differently in ECHAM6.1-HAM2.3.

Sedimentation is described in the two-moment microphysics as a bulk, size-averaged gravitational settling process based on the ice crystal radius and ambient atmospheric conditions (the atmospheric temperature, the pressure, and a height correction factor) (Spichtinger & Gierens, 2009). Ice crystals thus fall with a terminal fall velocity depending on their weight and the atmospheric conditions—note that sedimentation is only a downward-directed movement of ice crystals. The terminal fall velocity $v_{sedimented\ ice}$ is described by a power-law:

$$v_{\text{sedimented ice}} = C_{\text{vtfall}} \cdot \left(\rho_{\text{air}} \cdot q_{\text{i}}\right)^{0.16}, \tag{A3}$$

with an empirical sedimentation velocity coefficient C_{vtfall}, the density of air ρ_{air}, and the grid-box mean cloud ice mixing ratio q_{i}. The empirical sedimentation velocity coefficient C_{vtfall} captures the assumed mean ice particle habit, an implicit size–mass relationship, and the drag regime (Reynolds-number averaged). The product of the air density and the cloud ice mixing ratio is proportional to the ice mass concentration, so the fall speed increases weakly with increasing ice content, representing larger mean particle size and enhanced aggregation in ice-rich clouds.

Ice crystals can fall through several model levels until the ice crystal reaches the ground (and is added to the snow flux) or is sublimated on the way, based on the atmospheric conditions and height.

Vertical transport is calculated outside the two-moment microphysics, but instead comes from the dynamics scheme. It describes the vertical transport of ice crystals due to air movements. Vertical air movements that can transport ice crystals are, more explicitly, vertical advection, turbulence, and convective transport. Turbulence, however, is not resolved by the model. The effect of turbulence is therefore captured by a diffusive closure. To describe the net vertical transport due to turbulence, a parameterization for vertical diffusion represents the turbulent mixing and the net effect of turbulent eddies. Convective transport is described in Section A1 and not taken into account in this study.

Vertical advection and diffusion can transport ice crystals up and down. However, in the context of this study, it is the downward transport that matters in terms of distributing the cloud ice and influencing the *SLF*. The vertical transport of the ice crystal number concentration N_i via vertical advection and vertical diffusion can be calculated as follows:

$$\frac{\partial N_{\text{i}}}{\partial t}_{\text{adv}} = -w \frac{\partial N_{\text{i}}}{\partial z} \tag{A4}$$

$$\frac{\partial N_{\text{i}}}{\partial t}_{\text{diff}} = \frac{\partial}{\partial z}\left(K_z \frac{\partial N_{\text{i}}}{\partial z}\right) \tag{A5}$$

where w is the resolved wind and K_z the eddy diffusivity, which can be computed based on the turbulence scheme (turbulent kinetic energy TKE).

A4. Parameterization of the Wegener Bergeron Findeisen Process

Even though the Wegener Bergeron Findeisen process is not used as a factor in the factorial design of this study, it still influences the simulations when ice is present in the clouds and is an important detail of the two-moment cloud microphysics scheme. It is implemented in ECHAM6.1-HAM2.3 as a threshold process based on the vertical velocity w (Korolev, 2007). As long as the vertical velocity w is smaller than the threshold value w^* liquid water will evaporate and deposit on existing ice crystals (Wegener Bergeron Findeisen process). When the vertical velocity exceeds that threshold, liquid water and ice can co-exist. The threshold vertical velocity w^* is determined by the ice crystal number concentration and size of the ice crystals, supersaturation with respect to liquid water and ice, and a coefficient depending on temperature and pressure (Lohmann & Hoose, 2009).

A5. Parameterization of Depositional Growth of Ice Crystals

The depositional growth of ice crystals is calculated based on the supersaturation (with respect to ice) S_{rmi} and the effective ice particle radius r_{rmi}. It takes into account that diffusion limits the growth of the particles (physical resistance from heat and vapor diffusion; described via the diffusion heat coefficient $D(T,p)$ below).

Additionally, two correction factors are applied: one to account for kinetic non-continuum effects when particles are small (Fuchs correction F_{Fuchs}) and one to account for ventilation, which enhances deposition for falling particles due to the airflow (F_{vent}). Combining all the terms, the growth of the ice mass $\left(q_{rmi}\right)$ due to deposition can be written as:

$$\frac{\Delta q_{\text{i}}}{\Delta t} = 8 \cdot r_{\text{i}} \cdot (S_{\text{i}} - 1) \cdot N_{\text{i}} \cdot F_{\text{vent}} \cdot F_{\text{Fuchs}} \cdot D(T, p). \tag{A6}$$

A6. Description of Ice Hydrometeors

ECHAM6.1-HAM2.3 does not use the single ice category P3 scheme yet (Dietlicher et al., 2018), but instead has two categories of ice hydrometeors: cloud ice and snow. The mass mixing ratio and number concentration of cloud ice are prognostic. Ice crystals are described as hexagonal plates (Lohmann & Neubauer, 2018). The size of the ice crystals is estimated via an empirical relationship based on the ice mass following (Pruppacher & Klett, 2010):

$$r_{\text{i,eff}} = 0.5 \cdot 10^{4} \left(\frac{IWC \cdot b}{0.0376\, N_i} \right)^{0.302}, \tag{A7}$$

with N_i being the ice crystal number concentration in m−3, IWC the ice water content in g m^{-3} and b = g^{-1}. The mass based effective radius $r_{\text{i,eff}}$ is then converted to a physical particle radius r_{i}:

$$r_{\text{i}}[\mu\text{m}] = 10^{-6} \cdot c \cdot \left(-2261 + \sqrt{5113188 + 2809 \cdot r_{\text{i,eff}}^{3}} \right)^{\frac{1}{3}}, \tag{A8}$$

with c = µm. The size used within the microphysics and the radiation scheme is consistent.

Snow is diagnosed from cloud ice using conversion rates from Lin et al. (1983) and Murakami (1990) based on size. The conceptual size threshold is 40 µm, but this value is not explicitly checked (instead, the mass-based autoconversion formulas are used). Because snow is a diagnostic variable, it is removed within one time step from the atmospheric column. However, within this time step, snow can interact with the cloud droplets (leading to riming, which in turn creates snow) and the aerosol particles (wet scavenging). Snow can also evaporate or melt within that timestep.

A7. Parameterization of Secondary Ice Processes

In ECHAM6.1-HAM2.3, only one secondary ice process (Hallet-Mossop) is implemented. However, due to the inefficiency of this process shown in previous studies (Hoose et al., 2008), it is not used in the standard setup of the model to save computational time. Hence, it was not switched on for the simulations of this study. Note that there is a follow-up study that focuses on secondary ice processes (Frostenberg et al., 2026).

Appendix B: Global Annual Mean Values of Cloud Variables

Table B1
Global Annual Mean Values (Year 2000, Nudged, Rounded to Two Digits After the Comma)

Simulation	*LWP* [g/m^2]	*IWP* [g/m^2]	Large-scale precip. [mm/m^2]	Cloud cover [%]
Std	55.81	9.18	480.58	55.58
No MPC	109.76	5.96	469.27	62.43
No freez	57.10	9.10	478.38	55.68
Only freez	79.83	7.98	485.83	62.38
No vtrans	59.68	7.77	485.09	54.31
Only vtrans	95.65	9.56	485.25	69.54
No sed	74.24	9.30	486.66	69.00
Only sed	65.71	7.02	487.58	53.86

Appendix C: Global Annual Mean Values of *SLF*

Table C1
Global Annual Mean Values of SLF at Different Temperatures T (Year 2000, Nudged, Rounded to Two Digits After the Comma)

Simulation	*SLF* (−10°C)	*SLF* (−15°C)	*SLF* (−20°C)	*SLF* (−25°C)	*SLF* (−30°C)	*SLF* (−35°C)
Std	0.59	0.37	0.24	0.16	0.1	0.03
No MPC	1.00	1.00	1.00	1.00	1.00	0.48
No freez	0.59	0.40	0.27	0.20	0.14	0.04
Only freez	0.99	0.98	0.98	0.91	0.63	0.19
No vtrans	0.65	0.48	0.34	0.26	0.16	0.03
Only vtrans	0.94	0.90	0.82	0.72	0.62	0.25
No sed	0.91	0.84	0.72	0.56	0.39	0.12
Only sed	0.68	0.51	0.39	0.31	0.22	0.05

Appendix D: Global Annual Averaged Supercooled Liquid Fraction (*SLF*) at Different Temperatures (Thin Clouds and Cloud Tops)

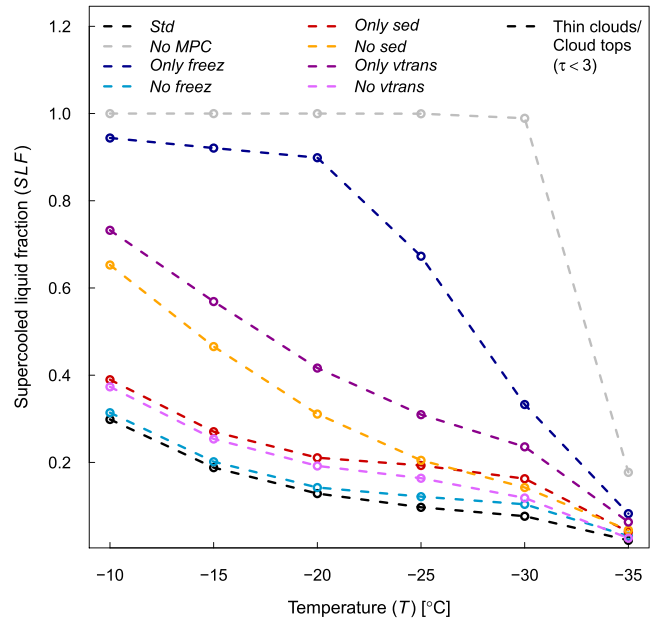

Figure D1. Global annual averaged supercooled liquid fraction (*SLF*) at different temperatures for all simulations for thin clouds and cloud tops ($\tau < 3$).

Conflict of Interest

The authors declare no conflicts of interest relevant to this study.

Availability Statement

The model output data from the GCM ECHAM6.1-HAM2.3 used for the analysis presented in this study are available at Zenodo (Ickes & Neubauer, 2025). The ECHAM-HAMMOZ model is developed by a consortium composed of ETH Zurich, Max Planck Institut für Meteorologie, Forschungszentrum Jülich, University of Oxford, the Finnish Meteorological Institute, and the Leibniz Institute for Tropospheric Research and managed by the Leibniz Institute for Tropospheric Research (TROPOS) (Ferrachat et al., 2026).

Acknowledgments

L.I. was supported by the Swiss National Science Foundation (Early Postdoc Mobility: grant no. 168886) and the Chalmers Gender Initiative for Excellence (Genie). David Neubauer and Ulrike Proske were supported by the European Union's Horizon 2020 research and innovation programme project FORCeS (grant agreement no. 821205). The authors thank Daniel Rieger for discussions, and special thanks go to Sylvaine Ferrachat for technical support with ECHAM6.1-HAM2.3. ECHAM-HAM simulations were performed on the ETH Zürich Euler cluster. The research presented in this paper is a contribution to the strategic research area "Modelling the Regional and Global Earth system," MERGE. Finally, we express our gratitude to the three anonymous reviewers for carefully reading our paper and for their valuable feedback.

References

Achtert, P., Seelig, T., Wallentin, G., Ickes, L., Shupe, M. D., Hoose, C., & Tesche, M. (2026). Occurrence of seeding multi-layer clouds in the Arctic from ground-based observations. *Atmospheric Chemistry and Physics*, *26*, 3049–3068. https://doi.org/10.5194/acp-26-3049-2026

Ansmann, A., Tesche, M., Seifert, P., Althausen, D., Engelmann, R., Fruntke, J., et al. (2009). Evolution of the ice phase in tropical altocumulus: SAMUM LiDAR observations over Cape Verde. *Journal of Geophysical Research*, *114*(D17), D17208. https://doi.org/10.1029/2008JD011659

Arakawa, A. (1975). Modelling clouds and cloud processes for use in climate models. In *WMO The Phys. Basis of Climate and Climate Modelling* (pp. 183–197). (SEE N 76-19675 10-47).

Arakawa, A. (2004). The cumulus parameterization problem: Past, present, and future. *Journal of Climate*, *17*(13), 2493–2525. https://doi.org/10.1175/1520-0442(2004)017⟨2493:RATCPP⟩2.0.CO;2

Barrett, A. I., Hogan, R. J., & Forbes, R. M. (2017a). Why are mixed-phase altocumulus clouds poorly predicted by large-scale models? Part 1. Physical processes. *Journal of Geophysical Research: Atmospheres*, *122*(18), 9903–9926. https://doi.org/10.1002/2016JD026321

Barrett, A. I., Hogan, R. J., & Forbes, R. M. (2017b). Why are mixed-phase altocumulus clouds poorly predicted by large-scale models? Part 2. Vertical resolution sensitivity and parameterization. *Journal of Geophysical Research: Atmospheres*, *122*(18), 9927–9944. https://doi.org/10.1002/2016JD026322

Bigg, E., & Meade, R. (1970). Ice nuclei active at low temperatures and humidities. *Bulletin of the American Meteorological Society*, *51*, 565. AMER METEOROLOGICAL SOC 45 BEACON ST, BOSTON, MA 02108-3693.

Bony, S., Colman, R., Kattsov, V. M., Allan, R. P., Bretherton, C. S., Dufresne, J.-L., et al. (2006). How well do we understand and evaluate climate change feedback processes? *Journal of Climate*, *19*(15), 3445–3482. https://doi.org/10.1175/JCLI3819.1

Boucher, O., Randall, D., Artaxo, P., Bretherton, C., Feingold, G., Forster, P., et al. (2013). Clouds and aerosols. In *Climate Change 2013: The Physical Science Basis. Contribution of Working Group I to the Fifth Assessment Report of the Intergovernmental Panel on Climate Change* (pp. 571–657). Cambridge University Press.

Braham, R. R., & Spyers-Duran, P. (1967). Survival of cirrus crystals in clear air. *Journal of Applied Meteorology*, *6*(6), 1053–1061. https://doi.org/10.1175/1520-0450(1967)006<1053:soccic>2.0.co;2

Bruno, O., Hoose, C., Storelvmo, T., Coopman, Q., & Stengel, M. (2021). Exploring the cloud top phase partitioning in different cloud types using active and passive satellite sensors. *Geophysical Research Letters*, *48*(2), e2020GL089863. https://doi.org/10.1029/2020GL089863

Carlsen, T., & David, R. O. (2022). Spaceborne evidence that ice-nucleating particles influence high-latitude cloud phase. *Geophysical Research Letters*, *49*(14), e2022GL098041. https://doi.org/10.1029/2022GL098041

Cesana, G., Waliser, D. E., Jiang, X., & Li, J.-L. F. (2015). Multimodel evaluation of cloud phase transition using satellite and reanalysis data. *Journal of Geophysical Research: Atmospheres*, *120*(15), 7871–7892. https://doi.org/10.1002/2014JD022932

Cess, R. D., Potter, G. L., Blanchet, J. P., Boer, G. J., Ghan, S. J., Kiehl, J. T., et al. (1989). Interpretation of cloud-climate feedback as produced by 14 atmospheric general circulation models. *Science*, *245*(4917), 513–516. https://doi.org/10.1126/science.245.4917.513

Chahine, M. T. (1992). The hydrological cycle and its influence on climate. *Nature*, *359*(6394), 373–380. https://doi.org/10.1038/359373a0

de Boer, G., Morrison, H., Shupe, M. D., & Hildner, R. (2011). Evidence of liquid dependent ice nucleation in high-latitude stratiform clouds from surface remote sensors. *Geophysical Research Letters*, *38*(1). https://doi.org/10.1029/2010GL046016

DeMott, P. J., Prenni, A. J., Liu, X., Kreidenweis, S. M., Petters, M. D., Twohy, C. H., et al. (2010). Predicting global atmospheric ice nuclei distributions and their impacts on climate. *Proceedings of the National Academy of Sciences*, *107*(25), 11217–11222. https://doi.org/10.1073/pnas.0910818107

Di, H., & Yuan, Y. (2024). The characteristics of cloud macro-parameters caused by the seeder–feeder process inside clouds measured by millimeter-wave cloud radar in Xi'an, China. *Atmospheric Chemistry and Physics*, *24*(10), 5783–5801. https://doi.org/10.5194/acp-24-5783-2024

Diehl, K., & Wurzler, S. (2004). Heterogeneous drop freezing in the immersion mode: Model calculations considering soluble and insoluble particles in the drops. *Journal of the Atmospheric Sciences*, *61*(16), 2063–2072. https://doi.org/10.1175/1520-0469(2004)061⟨2063:HDFITI⟩2.0.CO;2

Dietlicher, R., Neubauer, D., & Lohmann, U. (2018). Prognostic parameterization of cloud ice with a single category in the aerosol-climate model ECHAM(v6.3.0)-HAM(v2.3). *Geoscientific Model Development*, *11*(4), 1557–1576. https://doi.org/10.5194/gmd-11-1557-2018

Dietlicher, R., Neubauer, D., & Lohmann, U. (2019). Elucidating ice formation pathways in the aerosol–climate model ECHAM6-HAM2. *Atmospheric Chemistry and Physics*, *19*(14), 9061–9080. https://doi.org/10.5194/acp-19-9061-2019

Dufresne, J.-L., & Bony, S. (2008). An assessment of the primary sources of spread of global warming estimates from coupled atmosphere–ocean models. *Journal of Climate*, *21*(19), 5135–5144. https://doi.org/10.1175/2008JCLI2239.1

Eriksson, P., Baró Pérez, A., Müller, N., Hallborn, H., May, E., Brath, M., et al. (2026). Advancements and continued challenges in observations and global modelling of atmospheric ice mass. *Atmospheric Chemistry and Physics*, *26*(4), 2741–2768. https://doi.org/10.5194/acp-26-2741-2026

Ferrachat, S., Heinold, B., & Kubin, A. (2026). ECHAM-HAMMOZ [Software]. Retrieved from https://redmine.hammoz.ethz.ch/projects/hammoz

Flato, G., Marotzke, J., Abiodun, B., Braconnot, P., Chou, S. C., Collins, W., et al. (2014). Evaluation of climate models. In *Climate Change 2013: The Physical Science Basis. Contribution of Working Group I to the Fifth Assessment Report of the Intergovernmental Panel on Climate Change* (pp. 741–866). Cambridge University Press.

Frostenberg, H. C., Costa-Surós, M., Georgakaki, P., Proske, U., Sotiropoulou, G., May, E., et al. (2026). Large discrepancies in dominant microphysical processes governing mixed-phase clouds across climate models. *npj Climate and Atmospheric Science*, *9*(1), 75. https://doi.org/10.1038/s41612-026-01342-7

He, Y., Yi, F., Liu, F., Yin, Z., Yi, Y., Zhou, J., et al. (2022). Natural seeder-feeder process originating from mixed-phase clouds observed with polarization LiDAR and radiosonde at a mid-latitude plain site. *Journal of Geophysical Research: Atmospheres*, *127*(5), e2021JD036094. https://doi.org/10.1029/2021JD036094

Hofer, S., Hahn, L. C., Shaw, J. K., McGraw, Z. S., Bruno, O., Hellmuth, F., & Storelvmo, T. (2024). Realistic representation of mixed-phase clouds increases projected climate warming. *Communications Earth & Environment*, *5*(1), 1–12. https://doi.org/10.1038/s43247-024-01524-2

Hoose, C., Lohmann, U., Erdin, R., & Tegen, I. (2008). The global influence of dust mineralogical composition on heterogeneous ice nucleation in mixed-phase clouds. *Environmental Research Letters*, *3*(2), 025003. https://doi.org/10.1088/1748-9326/3/2/025003

Hoose, C., & Möhler, O. (2012). Heterogeneous ice nucleation on atmospheric aerosols: A review of results from laboratory experiments. *Atmospheric Chemistry and Physics*, *12*(20), 9817–9854. https://doi.org/10.5194/acp-12-9817-2012

Huang, W. T. K., Ickes, L., Tegen, I., Rinaldi, M., Ceburnis, D., & Lohmann, U. (2018). Global relevance of marine organic aerosol as ice nucleating particles. *Atmospheric Chemistry and Physics*, *18*(15), 11423–11445. https://doi.org/10.5194/acp-18-11423-2018

Ickes, L., & Neubauer, D. (2025). ECHAM6.1-HAM2.3 climate data to investigate the importance of ice-triggering processes in mixed-phase clouds [Dataset]. https://doi.org/10.5281/zenodo.16422802

Kanji, Z. A., Ladino, L. A., Wex, H., Boose, Y., Burkert-Kohn, M., Cziczo, D. J., & Krämer, M. (2017). Overview of ice nucleating particles. *Meteorological Monographs*, *58*(1), 1.1–1.33. https://doi.org/10.1175/AMSMONOGRAPHS-D-16-0006.1

Kay, J. E., L'Ecuyer, T., Chepfer, H., Loeb, N., Morrison, A., & Cesana, G. (2016). Recent advances in Arctic cloud and climate research. *Current Climate Change Reports*, *2*(4), 159–169. https://doi.org/10.1007/s40641-016-0051-9

Komurcu, M., Storelvmo, T., Tan, I., Lohmann, U., Yun, Y., Penner, J. E., et al. (2014). Intercomparison of the cloud water phase among global climate models. *Journal of Geophysical Research: Atmospheres*, *119*(6), 3372–3400. https://doi.org/10.1002/2013JD021119

Korolev, A. (2007). Limitations of the Wegener–Bergeron–Findeisen Mechanism in the evolution of mixed-phase clouds. *Journal of the Atmospheric Sciences*, *64*(9), 3372–3375. https://doi.org/10.1175/JAS4035.1

Korolev, A., & Leisner, T. (2020). Review of experimental studies of secondary ice production. *Atmospheric Chemistry and Physics*, *20*(20), 11767–11797. https://doi.org/10.5194/acp-20-11767-2020

Kraut, I. (2015). *Separating the aerosol effect in case of a "Medicane"* PhD thesis. Karlsruhe Institute of Technology.

Lau, K. M., & Wu, H. T. (2003). Warm rain processes over tropical oceans and climate implications. *Geophysical Research Letters*, *30*(24). https://doi.org/10.1029/2003GL018567

Li, Z.-X., & Le Treut, H. (1992). Cloud-radiation feedbacks in a general circulation model and their dependence on cloud modelling assumptions. *Climate Dynamics*, *7*(3), 133–139. https://doi.org/10.1007/BF00211155

Lin, Y.-L., Farley, R. D., & Orville, H. D. (1983). Bulk parameterization of the snow field in a cloud model. *Journal of Applied Meteorology and Climatology*, *22*(6), 1065–1092. https://doi.org/10.1175/1520-0450(1983)022⟨1065:BPOTSF⟩2.0.CO;2

Lohmann, U., & Diehl, K. (2006). Sensitivity studies of the importance of dust ice nuclei for the indirect aerosol effect on stratiform mixed-phase clouds. *Journal of the Atmospheric Sciences*, *63*(3), 968–982. https://doi.org/10.1175/JAS3662.1

Lohmann, U., & Hoose, C. (2009). Sensitivity studies of different aerosol indirect effects in mixed-phase clouds. *Atmospheric Chemistry and Physics*, *9*, 8917–8934. https://doi.org/10.5194/acp-9-8917-2009

Lohmann, U., & Neubauer, D. (2018). The importance of mixed-phase and ice clouds for climate sensitivity in the global aerosol–climate model ECHAM6-HAM2. *Atmospheric Chemistry and Physics*, *18*(12), 8807–8828. https://doi.org/10.5194/acp-18-8807-2018

Lohmann, U., Stier, P., Hoose, C., Ferrachat, S., Kloster, S., Roeckner, E., & Zhang, J. (2007). Cloud microphysics and aerosol indirect effects in the global climate model ECHAM5-HAM. *Atmospheric Chemistry and Physics*, *7*, 3425–3446. https://doi.org/10.5194/acp-7-3425-2007

Matus, A. V., & L'Ecuyer, T. S. (2017). The role of cloud phase in Earth's radiation budget. *Journal of Geophysical Research: Atmospheres*, *122*(5), 2559–2578. https://doi.org/10.1002/2016JD025951

McCoy, D. T., Tan, I., Hartmann, D. L., Zelinka, M. D., & Storelvmo, T. (2016). On the relationships among cloud cover, mixed-phase partitioning, and planetary albedo in GCMs. *Journal of Advances in Modeling Earth Systems*, *8*(2), 650–668. https://doi.org/10.1002/2015ms000589

Min, Q., Joseph, E., & Duan, M. (2004). Retrievals of thin cloud optical depth from a multifilter rotating shadowband radiometer. *Journal of Geophysical Research*, *109*(D2). https://doi.org/10.1029/2003JD003964

Montgomery, D. C. (2013). *Design and analysis of experiments* (8th ed. ed.). John Wiley & Sons, Inc.

Mülmenstädt, J., Sourdeval, O., Delanoë, J., & Quaas, J. (2015). Frequency of occurrence of rain from liquid-mixed-and ice-phase clouds derived from A-Train satellite retrievals. *Geophysical Research Letters*, *42*(15), 6502–6509. https://doi.org/10.1002/2015GL064604

Murakami, M. (1990). Numerical modeling of dynamical and microphysical evolution of an isolated convective cloud. *Journal of the Meteorological Society of Japan. Series II*, *68*(2), 107–128. https://doi.org/10.2151/jmsj1965.68.2_107

Neubauer, D., Ferrachat, S., Siegenthaler-Le Drian, C., Stier, P., Partridge, D. G., Tegen, I., et al. (2019). The global aerosol–climate model ECHAM6.3–HAM2.3—Part 2: Cloud evaluation, aerosol radiative forcing, and climate sensitivity. *Geoscientific Model Development*, *12*(8), 3609–3639. https://doi.org/10.5194/gmd-12-3609-2019

Proske, U., Bessenbacher, V., Dedekind, Z., Lohmann, U., & Neubauer, D. (2021). How frequent is natural cloud seeding from ice cloud layers (<35°C) over Switzerland? *Atmospheric Chemistry and Physics*, *21*(6), 5195–5216. https://doi.org/10.5194/acp-21-5195-2021

Proske, U., Ferrachat, S., Klampt, S., Abeling, M., & Lohmann, U. (2023). Addressing complexity in global aerosol climate model cloud microphysics. *Journal of Advances in Modeling Earth Systems*, *15*(5), e2022MS003571. https://doi.org/10.1029/2022MS003571

Pruppacher, H., & Klett, J. (2010). In L. A. Mysak & K. Hamilton (Eds.), *Microphysics of clouds and precipitation* (Vol. 18). Springer. https://doi.org/10.1007/978-0-306-48100-0

Quante, M. (2004). The role of clouds in the climate system. *Journal de Physique IV*, *121*, 61–86. https://doi.org/10.1051/jp4:2004121003

Ramelli, F., Henneberger, J., David, R. O., Bühl, J., Radenz, M., Seifert, P., et al. (2021). Microphysical investigation of the seeder and feeder region of an Alpine mixed-phase cloud. *Atmospheric Chemistry and Physics*, *21*(9), 6681–6706. https://doi.org/10.5194/acp-21-6681-2021

Sesartic, A., Lohmann, U., & Storelvmo, T. (2012). Bacteria in the ECHAM5-HAM global climate model. *Atmospheric Chemistry and Physics*, *12*, 8645–8661. https://doi.org/10.5194/acp-12-8645-2012

S. Solomon, & I. P. on Climate Change (Eds.) (2007)., *Climate Change 2007: The Physical Science Basis: Contribution of Working Group I to the Fourth Assessment Report of the Intergovernmental Panel on Climate Change*. Cambridge University Press. (OCLC: ocn132298563).

Spichtinger, P., & Gierens, K. M. (2009). Modelling of cirrus clouds—Part 1a: Model description and validation. *Atmospheric Chemistry and Physics*, *9*(2), 685–706. https://doi.org/10.5194/acp-9-685-2009

Stein, U., & Alpert, P. (1993). Factor separation in numerical simulations. *Journal of the Atmospheric Sciences*, *50*(14), 2107–2115. https://doi.org/10.1175/1520-0469(1993)050⟨2107:FSINS⟩2.0.CO;2

Storelvmo, T., Hoose, C., & Eriksson, P. (2011). Global modeling of mixed-phase clouds: The albedo and lifetime effects of aerosols. *Journal of Geophysical Research*, *116*(D5), D05207. https://doi.org/10.1029/2010JD014724

Tan, I., & Barahona, D. (2022). The impacts of immersion ice nucleation parameterizations on Arctic mixed-phase stratiform cloud properties and the arctic radiation budget in GEOS-5. *Journal of Climate*, *35*(13), 4049–4070. https://doi.org/10.1175/JCLI-D-21-0368.1

Tan, I., & Storelvmo, T. (2016). Sensitivity study on the influence of cloud microphysical parameters on mixed-phase cloud thermodynamic phase partitioning in CAM5. *Journal of the Atmospheric Sciences*, *73*(2), 709–728. https://doi.org/10.1175/JAS-D-15-0152.1

Tan, I., Storelvmo, T., & Zelinka, M. D. (2016). Observational constraints on mixed-phase clouds imply higher climate sensitivity. *Science*, *352*(6282), 224–227. https://doi.org/10.1126/science.aad5300

Tan, I., Zhou, C., Lamy, A., & Stauffer, C. L. (2025). Moderate climate sensitivity due to opposing mixed-phase cloud feedbacks. *npj Climate and Atmospheric Science*, *8*(1), 86. https://doi.org/10.1038/s41612-025-00948-7

Teller, A., & Levin, Z. (2008). Factorial method as a tool for estimating the relative contribution to precipitation of cloud microphysical processes and environmental conditions: Method and application. *Journal of Geophysical Research*, *113*(D2), D02202. https://doi.org/10.1029/2007JD008960

Terai, C. R., Klein, S. A., & Zelinka, M. D. (2016). Constraining the low-cloud optical depth feedback at middle and high latitudes using satellite observations. *Journal of Geophysical Research: Atmospheres*, *121*(16), 9696–9716. https://doi.org/10.1002/2016JD025233

Vassel, M., Ickes, L., Maturilli, M., & Hoose, C. (2019). Classification of Arctic multilayer clouds using radiosonde and radar data in Svalbard. *Atmospheric Chemistry and Physics*, *19*(7), 5111–5126. https://doi.org/10.5194/acp-19-5111-2019

Villanueva, D., Neubauer, D., Gasparini, B., Ickes, L., & Tegen, I. (2021). Constraining the impact of dust-driven droplet freezing on climate using cloud-top-phase observations. *Geophysical Research Letters*, *48*(11), e2021GL092687. https://doi.org/10.1029/2021GL092687

Waliser, D. E., Li, J.-L. F., Woods, C. P., Austin, R. T., Bacmeister, J., Chern, J., et al. (2009). Cloud ice: A climate model challenge with signs and expectations of progress. *Journal of Geophysical Research*, *114*(D8). https://doi.org/10.1029/2008jd010015

Wang, T., & Min, Q. (2008). Retrieving optical depths of optically thin and mixed-phase clouds from MFRSR measurements. *Journal of Geophysical Research*, *113*(D19). https://doi.org/10.1029/2008JD009958

Zelinka, M. D., Myers, T. A., McCoy, D. T., Po-Chedley, S., Caldwell, P. M., Ceppi, P., et al. (2020). Causes of higher climate sensitivity in cmip6 models. *Geophysical Research Letters*, *47*(1), e2019GL085782. https://doi.org/10.1029/2019GL085782

Zhang, K., O'Donnell, D., Kazil, J., Stier, P., Kinne, S., Lohmann, U., et al. (2012). The global aerosol-climate model ECHAM-HAM, version 2: Sensitivity to improvements in process representations. *Atmospheric Chemistry and Physics*, *12*(19), 8911–8949. https://doi.org/10.5194/acp-12-8911-2012